RESEARCH TITLE

Studying the Mechanism of Soot Reduction via Co-Combustion of Methane in a Laminar n-heptane Diffusion Flame

Nasreldin M. Mahmoud[1]

[1] Mechanical Engineering Department, Faculty of Engineering, University of Sinnar, Sinnar, Sudan
*Corresponding author. Mechanical Engineering Department, Faculty of Engineering, University of Sinnar, Sinnar, Sudan
E-mail address: nasrmohamed53@hotmail.com ; nasrmohamed@uofs.edu.sd.

Abstract

The combustion of n-heptane/methane mixtures in dual-fuel systems presents a promising strategy for reducing soot emissions, yet the underlying suppression mechanisms require further quantification. This study employs numerical simulation to investigate the structural and effects of methane addition on a laminar n-heptane diffusion flame. A validated coupled model, incorporating detailed chemical kinetics mechanism and a discrete sectional soot model, is applied. Simulations results reveal that methane blending significantly suppresses soot volume fraction, with the normalized peak value decreasing monotonically with methane addition. While the peak flame temperature remains stable, the entire thermal structure shifts toward the fuel nozzle due to altered mixture reactivity. Analysis of key intermediates shows that methane addition reduces peak concentrations of aromatic precursors, with a progressively stronger inhibition effect observed for larger polycyclic aromatic hydrocarbons. This size-dependent suppression indicates that methane chemically interferes with molecular growth processes beyond the first aromatic ring, likely through perturbation of the H-abstraction-C_2H_2-addition (HACA) mechanism and radical pool modification. The results elucidate the combined dilution and chemical effects governing soot reduction, providing critical insights for optimizing dual-fuel combustion towards minimal particulate emissions.

عنوان البحث

دراسة آلية تقليل تكوّن السناج من خلال الاحتراق المشترك للميثان في لهب انتشار صفحي لغاز-n هيبتان

المستخلص

يُعد احتراق خلطات –nهيبتان/الميثان في أنظمة الوقود المزدوج استراتيجية واعدة للحد من انبعاثات السناج، إلا أن الآليات الكامنة وراء هذا التثبيط لا تزال بحاجة إلى مزيد من التكميم والدراسة. توظف هذه الدراسة المحاكاة العددية للتحقق من البنية اللهبية وتأثيرات إضافة الميثان على لهب انتشار صفحي لـ –nهيبتان. وقد استُخدم نموذج مقترن تم التحقق من صحته، يدمج آلية حركية كيميائية تفصيلية مع نموذج مقطعي منفصل للسناج.

تُظهر نتائج المحاكاة أن مزج الميثان يثبط بشكل ملحوظ الكسر الحجمي للسناج، حيث تنخفض القيمة العظمى المعيارية بصورة رتيبة مع زيادة نسبة الميثان. وفي حين تبقى درجة حرارة اللهب العظمى شبه مستقرة، فإن البنية الحرارية الكاملة تتحول باتجاه فوهة الوقود نتيجة تغير تفاعلية الخليط. كما يكشف تحليل المتوسِّطات الكيميائية الرئيسة أن إضافة الميثان تقلل من القيم العظمى لتركيزات السوابق العطرية، مع ملاحظة تأثير تثبيطي متزايد كلما ازداد حجم الهيدروكربونات العطرية متعددة الحلقات.

يشير هذا التثبيط المعتمد على الحجم إلى أن الميثان يتداخل كيميائياً مع عمليات النمو الجزيئي لما بعد تكوّن الحلقة العطرية الأولى، ويرجَّح أن يكون ذلك من خلال إرباك آلية نزع الهيدروجين–إضافة الأسيتيلين (HACA) وتعديل تجمع الجذور الحرة. وتوضح هذه النتائج التأثيرات المشتركة للتخفيف والتداخل الكيميائي التي تتحكم في خفض تكوّن السناج، مما يوفر رؤى أساسية لتحسين احتراق الوقود المزدوج بهدف تقليل الانبعاثات الجسيمية إلى أدنى حد.

الكلمات المفتاحية: الاحتراق ثنائي الوقود؛ تكوّن السناج؛ الهيدروكربونات العطرية متعددة الحلقات(PAH) ؛ لهب الانتشار.

Introduction

Increasing global challenges, including oil shortages and air pollution, have highlighted the urgent need for advanced, sustainable power transmission solutions in the transportation industry [1]. In this context, natural gas (mainly methane) has emerged as a promising alternative fuel due to its abundant reserves, lower carbon-to-hydrogen ratio compared to conventional liquid hydrocarbons, and potential to reduce greenhouse gas and pollutant emissions [2]. Co-firing natural gas with traditional liquid fuels in dual-fuel combustion strategies offers a practical pathway for decarbonizing internal combustion engines and gas turbines. However, the fundamental chemical interactions between methane and higher hydrocarbons during combustion, particularly their combined impact on soot formation pathways, remain insufficiently quantified. Soot emissions are a critical concern for air quality and human health, and their formation is intricately linked to the complex pyrolysis chemistry of fuels, including the growth of polycyclic aromatic hydrocarbons (PAHs) [3]. This study investigates the structural and chemical effects of methane addition on a laminar diffusion flame of n-heptane (a common diesel surrogate) using detailed numerical simulation. The work specifically examines the evolution of flame temperature, key intermediate species, PAHs, and soot volume fraction to elucidate the chemical and physical mechanisms by which methane moderates soot production. Validations are performed against established experimental data to ensure model fidelity, providing insights critical for optimizing dual-fuel systems towards minimal particulate emissions.

Numerical Methodology

2.1 Burner Configurations

The counterflow diffusion flame configuration was selected for this study due to its well-defined, quasi-one-dimensional structure, which is highly amenable to detailed numerical simulation and provides a canonical framework for investigating soot kinetics. The configuration consists of two vertically opposed nozzles, with the fuel mixture n-heptane and methane issuing from the lower nozzle and the oxidizer (air) from the upper nozzle, separated by a distance of L. The simulations were performed using an opposed-flow module that solves the governing equations for mass, momentum, energy, and species conservation in an axisymmetric geometry [4]. By assuming a plug-flow velocity profile at the boundaries and a linear radial velocity variation, the system of partial differential equations can be reduced to a set of ordinary differential equations dependent solely on the axial coordinate. This one-dimensional approximation significantly enhances computational efficiency while retaining the essential physics for studying detailed chemistry and soot formation. Radiation heat loss from major gaseous species (CO, CO_2, H_2O, CH_4) and soot particles was accounted for using the optically thin approximation, neglecting self-absorption [5, 6]. A constant global strain rate of $K = 50$ s^{-1} was maintained for all simulated flames to ensure consistent aerodynamic conditions, with the nozzle exit velocities adjusted accordingly for different fuel compositions [7].

2.2. Chemical Kinetic Mechanism and Soot Model

The gas-phase kinetics were described by a detailed chemical mechanism developed for the combustion of practical fuel components, including a validated sub-mechanism for n-heptane oxidation [8]. This mechanism, comprising 291 species and 1223 elementary reactions, includes comprehensive PAH formation chemistry up to pyrene (A4). A well-established methane oxidation sub-mechanism was integrated to accurately capture its pyrolysis and oxidation pathways. Soot formation was modeled using a discrete sectional method (DSM) [9-11]. The particle size distribution was discretized into 30 sections, with the

volume of each successive section doubling that of the previous one. Soot inception was modeled via the dimerization of pyrene (A_4) molecules. Subsequent particle evolution was governed by key processes: surface growth via the hydrogen-abstraction-acetylene-addition (HACA) mechanism   [12, 13], physical condensation of gas-phase PAHs, particle coagulation in the free-molecular regime (enhanced by a Van der Waals factor of 2.2 [14]), and oxidation by O_2 and OH radicals. Oxidation rates by O_2 were adopted from established models [15], while a constant collision efficiency of $\gamma\_OH = 0.13$ was used for OH oxidation [16].

2.3. Boundary Conditions and Case Definition

The baseline condition simulates a diluted n-heptane/air flame, replicating the previous experimental setup [17, 18]. The fuel stream composition (mole fraction) was 0.4 C_7H_{16} and 0.6 N_2, while the oxidizer stream was composed of 0.21 O_2 and 0.79 N_2 (air). Both fuel and oxidizer inlet temperatures were fixed at 400 K. To investigate the effect of methane addition, n-heptane in the fuel stream was partially replaced by CH_4. The methane doping ratio, R_{CH4}, is defined as:

$$R_{CH_4} = \frac{x_{CH_4}}{x_{C_7H_{16}} + x_{CH_4}}$$

where x denotes mole fraction. The total mole fraction of the carbon-containing fuel (C_7H_{16} + CH_4) was kept constant at 0.4, with nitrogen making up the remaining 0.6 of the fuel streams. Cases with R_{CH_4} = 0 (pure n-heptane), 0.2, and 0.4 were simulated to gradually assess the impact of methane blending.

Model Validations and Flame Structure

Prior to analyzing the effects of methane addition, the predictive capability of the coupled gas-phase and soot models was rigorously validated against experimental data for the baseline n-heptane flame. Figure 3 presents the predicted flame structure for the baseline n-heptane (C_7H_{16}) flame, validated against experimental data [17, 18]. Panel (a) shows excellent agreement between predicted and measured temperature profiles along the central axis, confirming the model's accuracy in capturing thermal characteristics. As expected, n-heptane fuel concentration decreases monotonically from the nozzle, depleting entirely at the flame sheet (coincident with the peak temperature, ($X_{T,max}$), while oxygen concentration diminishes from the oxidizer side. Critical pyrolysis intermediates such as C_2H_2 and C_3H_3 are present exclusively on the fuel-rich side, serving as vital precursors for PAH formation [6]. Panel (b) illustrates the spatial distribution of aromatic species (A1: benzene, A2: naphthalene, A3: phenanthrene, A4: pyrene) and the computed soot volume fraction (SVF). The peak concentrations of PAHs are located within the high-temperature region, consistent with established understanding that PAH growth is thermally promoted [19-22]. The predicted SVF profile and its peak magnitude align well with the experimental measurements [17, 18], although a slight spatial discrepancy in the peak location is observed, potentially attributable to uncertainties in the soot model's treatment of particle transport or oxidation.
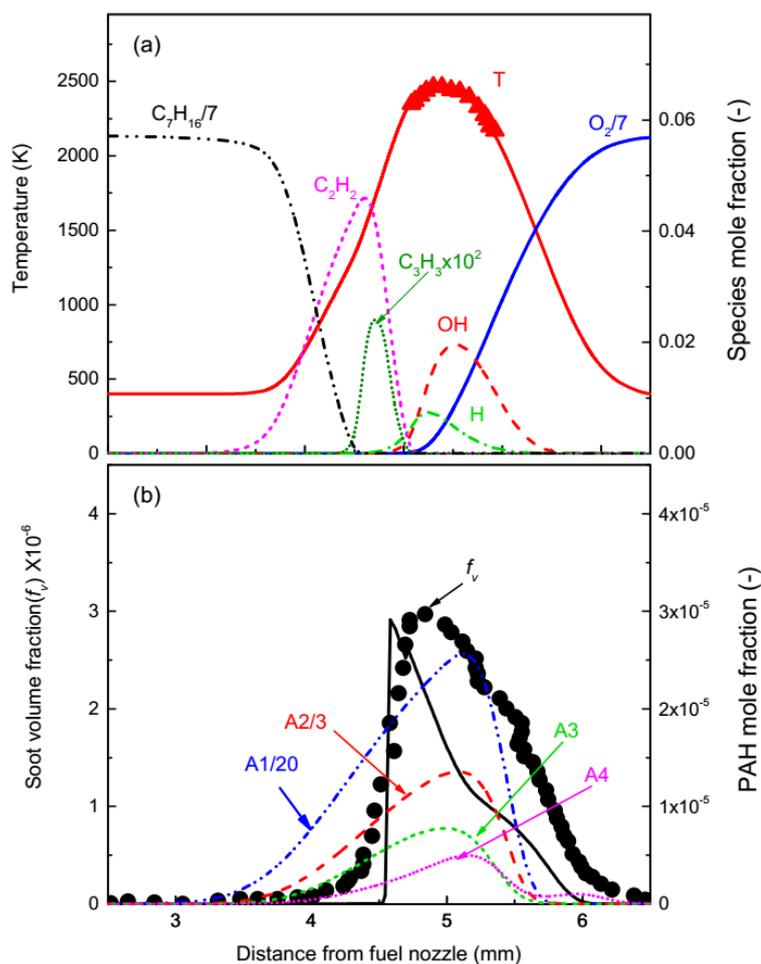
Figure 3. Predicted flame structures of baseline C_7H_{16} flame; (a) flame temperature and relevant important species profiles; (b) the computed soot volume fraction profiles along with A1, A2, A3, and A4. The experimental results of temperature and soot volume fraction adopted from [17, 18] are also plotted for validations (symbols).

Figure 5 compares the soot volume fraction for pure n-heptane and n-heptane/methane mixture flames. Panel (a) demonstrates that methane addition consistently reduces the spatial SVF profile. Panel (b) quantifies this effect through the normalized maximum SVF, revealing a suppression of soot formation with increasing methane doping ratio. This suppression can be attributed to a combination of dilution and chemical effects. Methane, being a single-carbon molecule, dilutes the pool of available soot precursors from n-heptane pyrolysis. Furthermore, its stable C-H bonds and distinct pyrolysis pathways can chemically inhibit the growth of larger aromatic clusters by altering the H-abstraction-C_2H_2-addition (HACA) reaction pathway or competing for key radicals [20, 21, 23, 24]. The observed trend is consistent with previous studies on hydrocarbon blending effects on soot yields [25] .
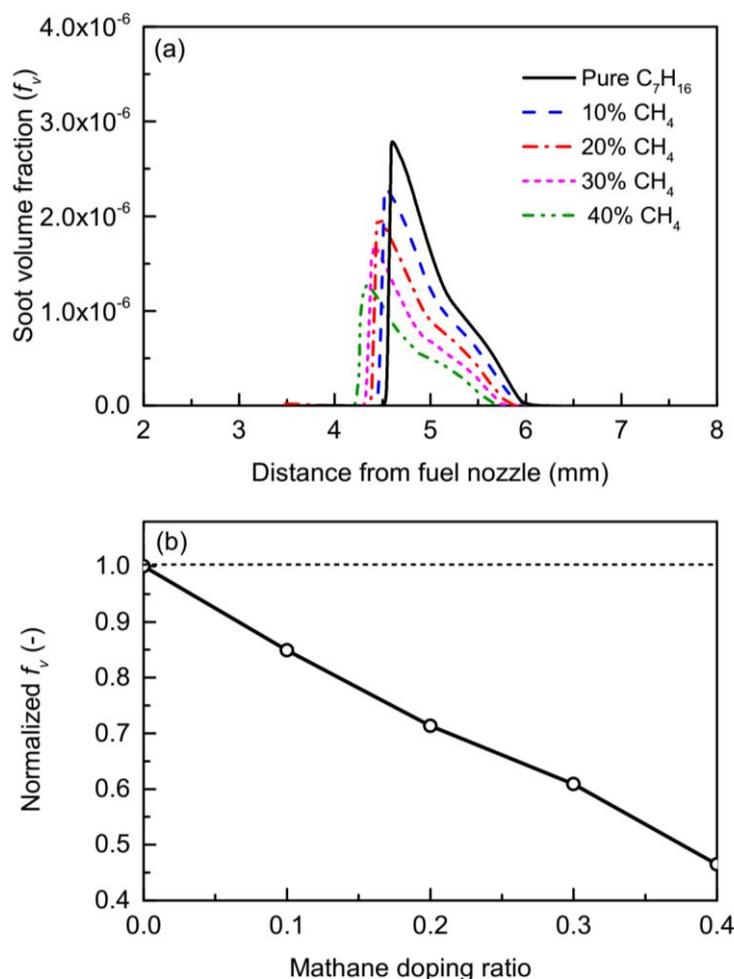
Figure 4. Comparison of soot volume fraction profile (a) and normalized max of (f_v) (b) of n-heptane with increasing methane blending ratio.

The influence of methane addition on flame temperature is a critical factor, as temperature governs pyrolysis, oxidation, and soot formation kinetics [26]. The results indicate that the peak flame temperature remains largely unchanged with methane blending. However, the entire temperature profile shifts spatially towards the fuel nozzle. This shift is likely a consequence of the altered fuel stream momentum and reactivity of the mixture; methane's different ignition delay and lower adiabatic flame temperature can modify the local stoichiometry and heat release distribution [24, 27]. This thermal field shift has direct implications for precursor chemistry, as evidenced in the subsequent analysis of PAHs.
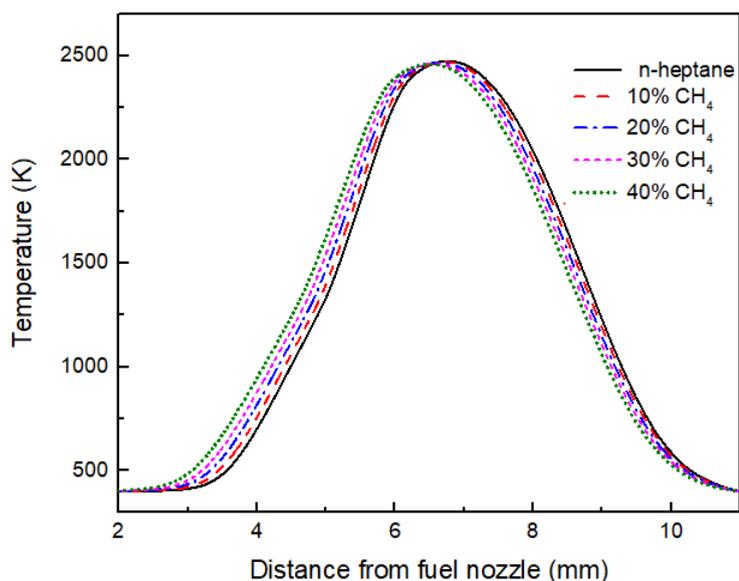
Fig.5 Flame temperature of n-heptane with increasing methane blending ratio.

The effect of adding 40% CH_4 to heptane on the calculated aromatic species profiles is compared in Fig. 6. As shown in the figure, the peak concentration of A1 shows a decrease with the addition of 40% CH_4. The suppression effect of CH_4 addition becomes progressively more pronounced for larger PAHs (I,e A2-A4). This size-dependent inhibition strongly suggests that methane addition interferes with the molecular growth processes beyond the first aromatic ring. The chemical mechanism likely involves the perturbation of reaction sequences leading from A1 to A4, possibly through the aforementioned modification of the HACA mechanism or via the provision of additional H-atoms that terminate growth [22, 24, 26, 28]. Notably, the spatial profiles of all aromatic species shift towards the fuel nozzle in tandem with the temperature profile shift, reinforcing the linkage between the altered thermal structure and the chemistry of soot precursor formation.
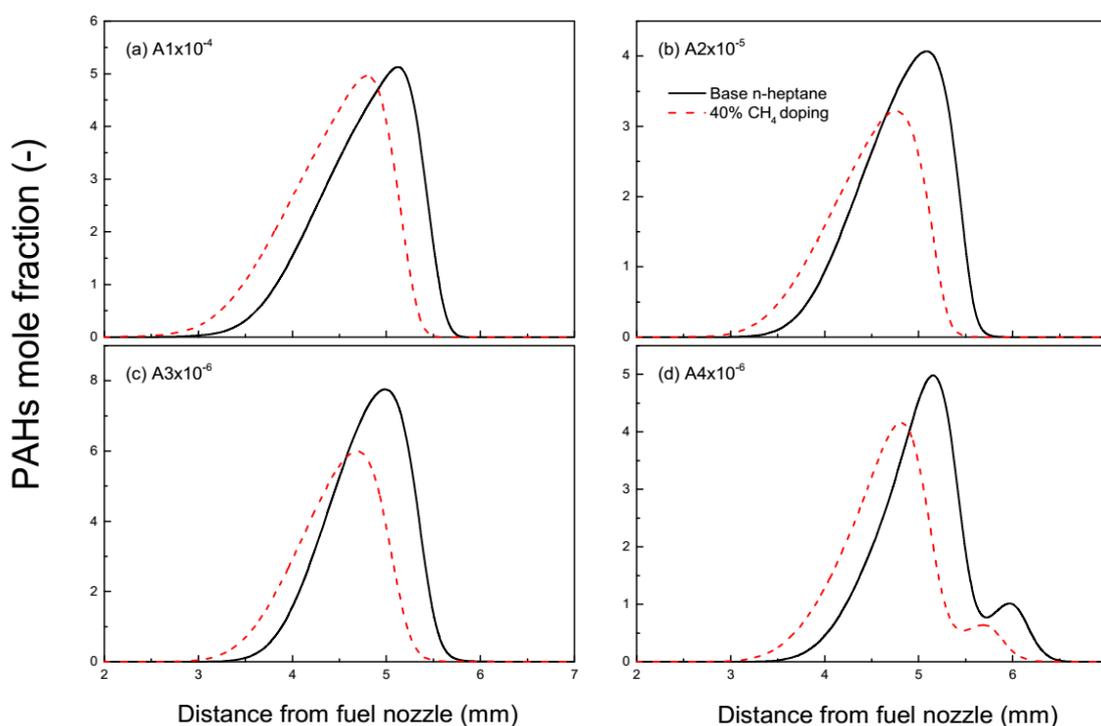

Fig.6 Benzene and PAHs formation of n-heptane with 40% of methane blending ratio.

Conclusions

This numerical investigation elucidates the impact of methane addition on soot formation pathways in a laminar n-heptane diffusion flame. The coupled gas-phase and soot model demonstrated good predictive capability against experimental data for the baseline n-heptane flame. The key finding is that methane blending consistently suppresses soot formation, as quantified by the reduction in peak soot volume fraction with increasing methane doping ratio. This suppression is attributed to a combination of dilution of soot precursors from n-heptane pyrolysis and basic chemical effects. The chemical role of methane is elucidated through the analysis of flame structure and precursor formation. Although the peak flame temperature is largely unaffected, the spatial shift of the thermal field influences precursor formation zones. More significantly, methane addition inhibits the formation of larger PAHs, with the suppression effect becoming more pronounced for larger aromatic species like pyrene (A4). This trend strongly suggests that methane actively inhibits with the growth chemistry responsible for building larger PAHs, which are critical soot inception precursors. The mechanism likely involves the alteration of the HACA reaction pathway and competition for key radical species. These results indicate that methane is not only a diluent but also a chemical inhibiter that alter the reaction chain from small hydrocarbons to soot precursors.

Acknowledgments

References

[1]   Korakianitis T, Namasivayam AM, Crookes RJ. Natural-gas fueled spark-ignition (SI) and compression-ignition (CI) engine performance and emissions. Progress in Energy and Combustion Science 2011;37(1):89-112.

[2]   Mac Kinnon MA, Brouwer J, Samuelsen S. The role of natural gas and its infrastructure in mitigating greenhouse gas emissions, improving regional air quality, and renewable resource integration. Progress in Energy and Combustion Science 2018;64:62-92.

[3]   Frenklach M. Reaction mechanism of soot formation in flames. Physical Chemistry Chemical Physics 2002;4.

[4]   CHEMKIN 15151, ANSYS Reaction Design: San Diego, . Reaction Design. 2016.

[5]   Hall RJ. The radiative source term for plane-parallel layers of reacting combustion gases. Journal of Quantitative Spectroscopy and Radiative Transfer 1993;49(5):517-23.

[6]   Ju Y, Guo H, Maruta K, Liu F, Ju Y, Maruta K. On the Extinction Limit and Flammability Limit of Non-Adiabatic Stretched Methane–air Premixed Flames. Journal of Fluid Mechanics 1997;342(342):315-34.

[7]   Seshadri K, Williams FA. Laminar flow between parallel plates with injection of a reactant at high reynolds number. International Journal of Heat and Mass Transfer 1978;21(2):251-3.

[8]   An Y-z, Pei Y-q, Qin J, Zhao H, Li X. Kinetic modeling of polycyclic aromatic hydrocarbons formation process for gasoline surrogate fuels. Energy Conversion and Management 2015;100:249-61.

[9]   Veshkini A, Eaves NA, Dworkin SB, Thomson MJ. Application of PAH-condensation reversibility in modeling soot growth in laminar premixed and nonpremixed flames. Combustion and Flame 2016;167:335-52.

[10]   Sirignano M, Kent J, D'Anna A. Modeling Formation and Oxidation of Soot in Nonpremixed Flames. Energy & Fuels 2013;27(4):2303-15.

[11]   Pejpichestakul W, Frassoldati A, Parente A, Faravelli T. Kinetic modeling of soot formation in premixed burner-stabilized stagnation ethylene flames at heavily sooting condition. Fuel 2018;234:199-206.

[12]   Wang Y, Raj A, Chung SH. Soot modeling of counterflow diffusion flames of ethylene-based binary mixture fuels. Combustion and Flame 2015;162(3):586-96.

[13]   Blanquart G, Pitsch H. Analyzing the effects of temperature on soot formation with a joint volume-surface-hydrogen model. Combustion and Flame 2009;156(8):1614–26.

[14]   Harris SJ, Kennedy IM. The Coagulation of Soot Particles with van der Waals Forces. Combustion Science and Technology 1988;59(4-6):443-54.

[15]   Celnik MS, Sander M, Raj A, West RH, Kraft M. Modelling soot formation in a premixed flame using an aromatic-site soot model and an improved oxidation rate. Proceedings of the Combustion Institute 2009;32(1):639-46.

[16]   Appel J, Bockhorn H, Frenklach M. Kinetic modeling of soot formation with detailed chemistry and physics: laminar premixed flames of C 2 hydrocarbons. Combust Flame 2000;121(1–2):122-36.

[17]   Nobili A, Zheng D, Pelucchi M, Cuoci A, Frassoldati A, Hui X, et al. Oxygen effects on soot formation in H2/n-heptane counterflow flames. Combustion and Flame 2023;253:112821.

[18]   Zheng D, Nobili A, Cuoci A, Pelucchi M, Hui X, Faravelli T. Soot formation from n-heptane counterflow diffusion flames: Two-dimensional and oxygen effects. Combustion and Flame 2023;258:112441.

[19]   Richter H, Howard JB. Formation of polycyclic aromatic hydrocarbons and their growth to soot—a review of chemical reaction pathways. Progress in Energy and Combustion Science 2000;26(4):565-608.

[20]   Mahmoud NM, Zhong W, Abdalla T, Wang Q, Edreis EMA. Chemical Effects of CO2 and H2O Addition on Aromatic Species in Ethanol/Air Diffusion Flame. Combustion Science and Technology 2020:1-19.

[21]   Mahmoud NM, Zhong W, Ibrahim JN, Wang Q. Flame Structure and Soot-Precursor Formation of Coflow n-Heptane Diffusion Flame Burning in O2/N2 and O2/CO2 Atmosphere. Journal of Energy Engineering 2021;147(4):04021027.

[22]   Mahmoud NM, Zhong W, Wang Q, He Z. Impact of n-butanol addition to hydrogenated catalytic biodiesel fueled a constant volume combustion chamber; a computational study. Energy Sources, Part A: Recovery, Utilization, and Environmental Effects 2023;45(4):12553-69.

[23]   Mahmoud NM, Yan FW, Zhou MX, Xu L, Wang Y. Coupled Effects of Carbon Dioxide and Water Vapor Addition on Soot Formation in Ethylene Diffusion Flames. Energy & Fuels 2019;33(6):5582-96.

[24]   Mahmoud NM. Numerical Study of Flame Structure and Precursors Formation of propane–H2 Mixtures. Humanities & Natural Sciences Journal 2025;6(12):549-57.

[25]   Liu F, Guo H, Smallwood GJ, Gülder ÖL. The Chemical Effects of Carbon Dioxide as an Additive in an Ethylene Diffusion Flame: Implications for Soot and NOx Formation. combustion and flame 2001;125:778-87.

[26]   Mahmoud NM, Yan F, Wang Y. Effects of fuel inlet boundary condition on aromatic species formation in coflow diffusion flames. Journal of the Energy Institute 2019;92(2):288-97.

[27]   Kirkpatrick AT, Kuo KK. Principles of combustion. John Wiley & Sons; 2024.

[28]   Mahmoud NM, Zhong W, Wang Q, Yuan Q, He Z. On the effect of injection pressure on spray combustion and soot formation processes of gasoline/second generation biodiesel blend. Therm Sci 2024;28(00):3967-78.